Performance Evaluation of a Distance Relay as Applied to a Transmission System With UPFC

Xiaoyao Zhou, Haifeng Wang, *Senior Member, IEEE*, R. K. Aggarwal, *Senior Member, IEEE,*, and Phil Beaumont, *Senior Member, IEEE*

***Abstract*—This paper presents analytical and simulation results of the application of distance relays for the protection of transmission systems employing flexible alternating current transmission controllers such as the unified power flow controller (UPFC). Firstly a detailed model of the UPFC and its control is proposed and then it is integrated into the transmission system for the purposes of accurately simulating the fault transients. An apparent impedance calculation procedure for a transmission line with UPFC based on the power frequency sequence component is then investigated. The simulation results show the impact of UPFC on the performance of a distance protection relay for different fault conditions; the studies also include the influence of the setting of UPFC control parameters and the operational mode of UPFC.**

***Index Terms*—Distance relay, flexible alternating current transmission (FACTS) controllers, power system protection, UPFC.**

I. Introduction

CONTINUING pressure to minimize capital expenditure and the increasing difficulties involved in obtaining transmission rights of way have focused the attention of the utility community on the flexible alternating current transmission (FACTS) concept [1], [2] resulting in the initiation of studies and implementation programmes which are now well underway. Power transfer in most integrated transmission systems is constrained by transient stability, voltage stability, and/or power stability. These constrains limit the full utilization of available transmission corridors. FACTS is a technology that provides the requisite corrections of transmission functionality in order to fully utilize existing transmission systems and, therefore, minimize the gap between the stability and thermal limits.

FACTS technology is based on the use of reliable high-speed power electronics, advanced control technology, high-power microcomputers and powerful analytical tools. The key feature is the availability of power electronic switching devices that can switch electricity at megawatt levels (kV and kA levels). The impact of FACTS controllers on transmission systems is thus likely to have a significant impact on power system networks worldwide.

Manuscript received February 17, 2005; revised July 4, 2005. Paper no. TPWRD-00090-2005.

X. Zhou, H. Wang, and R. K. Aggarwal are with the Department of Electronic and Electrical Engineering, University of Bath, Bath BA2 7AY U.K. (e-mail: eepxz@bath.ac.uk; eeshw@bath.ac.uk; R.K.Aggarwal@bath.ac.uk).

P. Beaumont is with Toshiba International (Europe) Ltd., Durham DH1 3UZ, U.K.

Digital Object Identifier 10.1109/TPWRD.2005.861329

Amongst the different types of FACTS controllers, UPFC is considered to be one of the most effective in the control of power flow. It comprises two back-to-back gate-turn-off thyristor (GTO) based voltage source converters (VSCs) connected by a dc -link capacitor. An exciting transformer connecting one VSC is arranged in shunt and a boosting transformer linking the second VSC is inserted into the transmission line. By virtue of its ability to control freely and independently three major parameters in power transmission *viz.* the line impedance and the magnitude and phase of the voltage, it provides both voltage regulation and improvement in stability.

Because of the presence of FACTS controllers in a fault loop, the voltage and current signals at the relay point will be affected in both the steady state and the transient state. This in turn will affect the performance of existing protection schemes, such as the distance relay which is one of the very widely used methods in transmission line protection [3], [4]. The main principle of this technique is to calculate the impedance between the relay and fault points; the apparent impedance is then compared with the relay trip characteristic to ascertain whether it is an internal or external fault. A common method of calculating this impedance is to use symmetrical component transformation using power frequency components of voltage and current signals measured at the relay point.

Some research has been done to evaluate the performance of a distance relay for transmission systems with FACTS controllers. The work in [5] has presented some analytical results based on steady-state model of STATCOM, and the authors have studied the impact of STATCOM on a distance relay at different load levels. In [6], the voltage-source model of FACTS controllers has been employed to study the impact of FACTS on the tripping boundaries of distance relay. The work in [7] shows that thyristor-controlled series capacitor (TCSC) has a major influence on the mho characteristic, in particular the reactance and directional characteristic, making the protected region unstable. The study in [8] also shows that the presence of FACTS controllers in a transmission line will affect the trip boundary of a distance relay, and both the parameters of FACTS controllers and their location in the line have an impact on the trip boundary. All the studies clearly show that when FACTS controllers are in a fault loop, their voltage and current injections will affect both the steady state and transient components in voltage and current signals, and hence the apparent impedance seen by a conventional distance relay is different from that for a system without FACTS. Although the work presented in the [6] and [8] show the adverse impact of FACTS controllers on the performance of distance relay, the models employed for the various

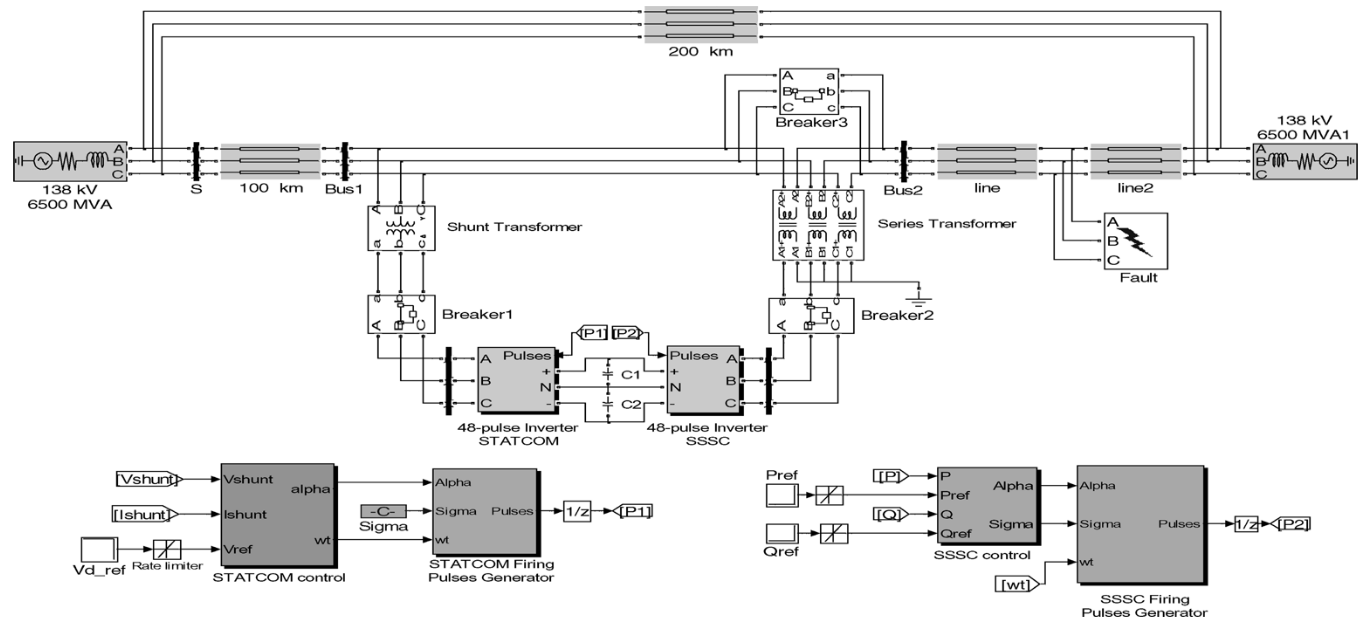

Fig. 1. Transmission system with UPFC.

FACTS controllers are rather simple and approximate and hence the studies are not an accurate reflection of the behavior of the distance relay in the FACTS environment.

The first part of this paper is to set up a very accurate model of a UPFC system including its complex control strategies, which is then embedded into a transmission system model; the simulated voltage and current signals at the relay point are then employed to make a comprehensive assessment of the performance of a typical distance relay protection under a vast majority of different system and fault conditions. The 138-kV transmission system employed herein is a typical system as encountered in the U.S. power system network.

II. UPFC and Transmission System Model

A. Transmission System Employing a UPFC Model

In this study, SimPowerSystem 3.1 toolbox in Matlab 7 is used to model the 138-kV parallel transmission system with UPFC installed in the middle of one transmission line [9]. The system built with this tool is shown in Fig. 1. Two 200-km parallel 138-kV transmission lines terminated in two 6500-MVA short-circuit levels (SCLs) sources and the angle difference is 20°. The 160-MVA UPFC is installed in the middle of the second transmission line. The simulation time step length is 0.02 ms.

The UPFC consists of two 48-pulse voltage source inverters which are connected through two 2000 μF common dc capacitors. The first inverter known as STATCOM connects into the transmission system through a 15 kV/138 kV Δ/Y shunt transformer, and injects or consumes reactive power to the transmission system to regulate the voltage at the connecting point; another inverter known as static synchronous series compensator (SSSC) connects into the system through a 15 kV/22 kV Y/Y series transformer to inject an almost sinusoidal voltage of variable magnitude and angle, in series with the transmission line to regulate the power flow through the transmission line.

The transmission line is based on the distributed parameter line model. The positive and negative sequence line impedance is $0.195+\mathrm{j}3.3425\ \mathrm{ohm/km}$, and the zero sequence transmission line impedance is $2.638+\mathrm{j}11.27\ \mathrm{ohm/km}$.

B. Voltage Source Inverter Model

The voltage source inverter employed herein is based on the 48-pulse quasiharmonic neutralized GTO inverter [10] and the structure is shown in Fig. 2. It consists of four 3-phase, 3-level GTO inverters and four phase-shifting transformers. Each inverter uses a 3-level GTO bridge block to generate three square-wave voltages. These voltage are fed to the secondary windings of four phase-shifting transformers whose primary windings are connected in series to produce an almost sinusoidal voltage output. A dc capacitor is connected to the four 3-level inverters, the magnitude of square-wave voltage can be $+\mathrm{V_{dc}}$, 0, $-\mathrm{V_{dc}}$. The duration of zero voltage in each quarter cycle is defined as "dead angle" γ, and it can be adjusted from 0°–90°. The fundamental component of voltage source inverter has the amplitude of

$$V_{X,n} = \frac{2}{\pi} V_{\mathrm{dc}} \cos\left(\frac{\pi}{24}\right) \cos\gamma. \tag{1}$$

As seen from above, the magnitude of the output voltage can be adjusted through changing the value of dead angle γ and/or the dc voltage of the capacitor. The phase angle α of the output voltage can be adjusted by using the input signal from the pulse generator. When the dead angle $\gamma=\pi/48$, the first significant harmonics of the voltage source inverter on the ac output are 47th and 49th and it is operated as a 48-pulse inverter. In this study, the STATCOM inverter is operated as 48-pulse inverter, that is to say, the dead angle kept constant during the operation, and the SSSC inverter is operated with a variable dead angle to control the amplitude of the injection voltage.

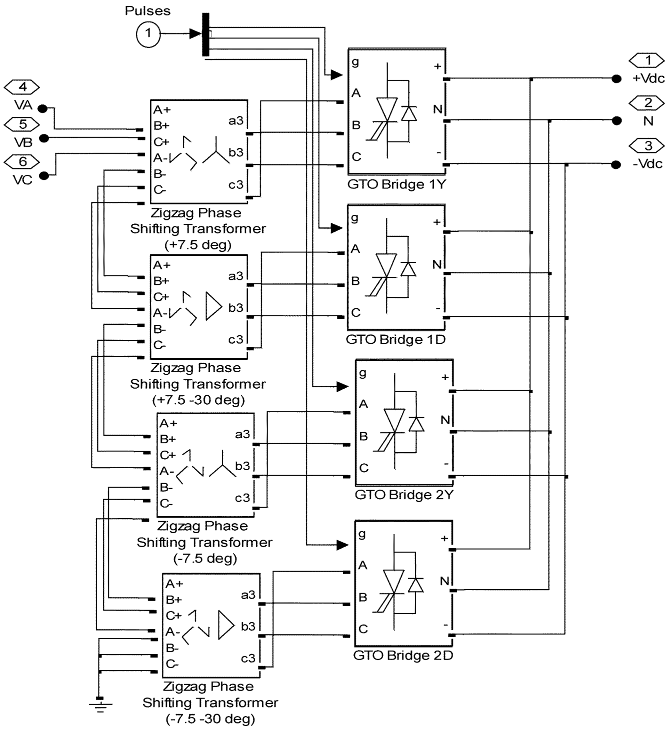

Fig. 2. 48-pulse quasi-harmonic neutralized GTO inverter.

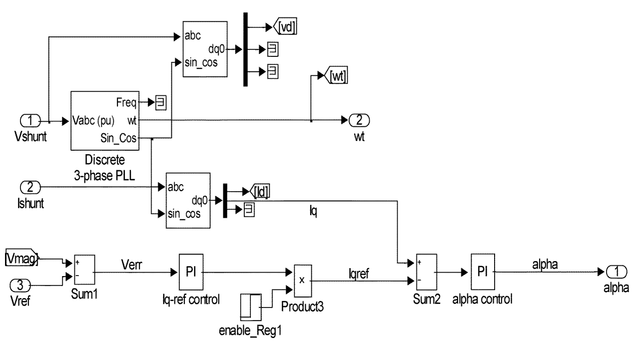

Fig. 3. Control model of STATCOM.

C. UPFC Control Model

The control system of the UPFC can be divided into two parts: the control of STATCOM and the control of SSSC. The control of STATCOM (Fig. 3) is used to operate the voltage source inverter to inject or absorb reactive power to regulate the connecting point voltage to the setting value $V_{\rm ref}$. The three phase voltages at the connecting point are sent to the Phase-Lock-Loop to calculate the reference angle which is synchronized to the phase A voltage. The three phase currents of STATCOM are decomposed into their real part I_d and reactive part I_q via the *abc-dqo* transform using the phase-lock-loop angle as reference. The magnitude of the positive sequence component of the connecting point voltage is compared with the desired reference voltage $V_{\rm ref}$, and the error is passed through a PI controller to produce the desired reactive current $I_{\rm qref}$; this current reference is compared with the reactive part of the shunt current to produce the error which will be passed through another PI controller to obtain the relative phase angle α of the inverter voltage with respect to the phase A voltage. The phase angle together with the phase-lock-loop signal are fed to the STATCOM firing pulse generator to generate the desired pulse for the voltage source inverter (the dead angle of STATCOM is kept fixed as $\gamma = \pi/48$).

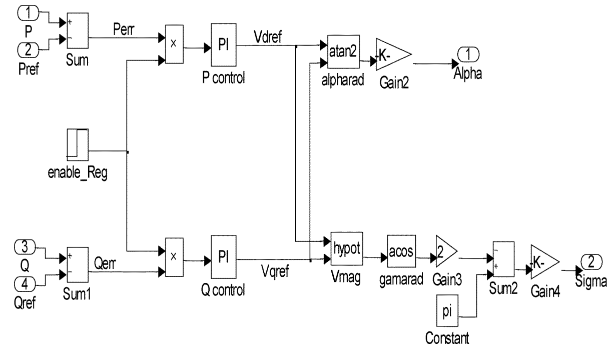

Fig. 4. Control model of SSSC.

The control strategy for the SSSC is based on automatic power flow control (Fig. 4). The series injected voltage is determined by a closed-loop control system to ensure that the desired active and reactive powers flowing in the transmission line are maintained despite power system changes. The desired $P_{\rm ref}$ and $Q_{\rm ref}$ are compared with the measured positive active and reactive power flows in the transmission line, and the errors are used to derive the desired direct and quadrature component of the series inverter voltage, $V_{\rm dref}$ and $V_{\rm qref}$,, respectively, through the PI controllers. The magnitude V_{pq} and phase angle α of series converter voltage can be obtained by a rectangular to polar transformation of $V_{\rm dref}$ and $V_{\rm qref}$ component. The dead angle of SSSC inverter can be calculated using the relationships between V_{pq} and dc capacitor voltage $V_{\rm dc}$, hence the phase angle α, dead angle γ together with the phase-lock-loop signal are used by the SSSC firing pulse generator to generate the desired pulse for the SSSC voltage source inverter.

III. Apparent Impedance Analysis

For the analysis of the operation of a distance relay, the power system shown in Fig. 1 is used; the relay is installed on the right side of Bus S. The apparent impedance calculation is based on symmetrical component transformation using power frequency components of voltage and current signals measured at the relay point.

A. Apparent Impedance Calculation

When a single phase-to-ground fault occurs on the right side of the UPFC and the distance is $n * L$ from the relay point, the positive, negative and zero sequence networks of the system during the fault are as shown in Fig. 5

$$V_{1s} = I_{1s}0.5Z_1 + V_{1pq} + I_{1\rm line}(n-0.5)Z_1 + R_fI_{1f} \quad (2)$$

$$V_{2s} = I_{2s}0.5Z_1 + V_{2pq} + I_{2\rm line}(n-0.5)Z_1 + R_fI_{2f} \quad (3)$$

$$V_{0s} = I_{0s}0.5Z_0 + V_{0pq} + I_{0\rm line}(n-0.5)Z_0 + R_fI_{0f} \quad (4)$$

$$I_{1\rm line} = I_{1s} + I_{1\rm sh} \quad (5)$$

$$I_{2\rm line} = I_{2s} + I_{2\rm sh} \quad (6)$$

$$I_{0\rm line} = I_{0s} + I_{0\rm sh} \quad (7)$$

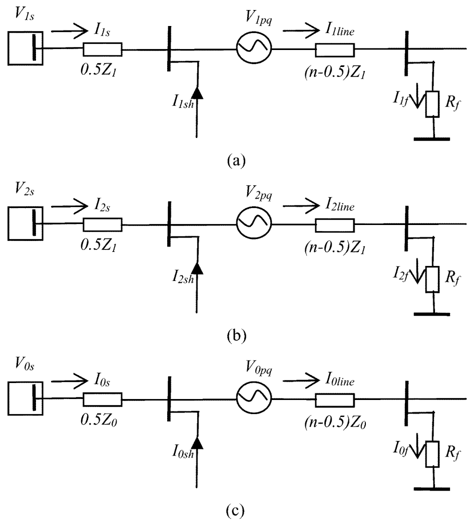

Fig. 5. Sequence networks of the system from the relay location to fault. (a) Positive sequence network. (b) Negative sequence network. (c) Zero sequence network.

where

V_{1s},V_{2s},V_{0s}	sequence phase voltages at the relay location;
V_{1pq},V_{2pq},V_{0pq}	series sequence phase voltages injected by UPFC;
I_{1s},I_{2s},I_{0s}	sequence phase currents at the relay location;
$I_{1\text{line}}$, $I_{2\text{line}}$, $I_{0\text{line}}$	sequence phase currents in transmission line;
I_{1f},I_{2f},I_{0f}	sequence phase currents in the fault;
$I_{1\text{sh}}$,$I_{2\text{sh}}$,$I_{0\text{sh}}$	shunt sequence phase currents injected by UPFC;
Z_1, Z_0	sequence impedance of the transmission line;
n	per-unit distance of a fault from the relay location.

From above, the voltage at the relay point can be derived as

$$V_s = nI_sZ_1 + nI_{0s}(Z_0 - Z_1) + I_{\text{sh}}(n-0.5)Z_1 + (n-0.5)I_{0\text{sh}}(Z_0 - Z_1) + V_{pq} + R_fI_f \quad (8)$$

where

$$V_s = V_{1s} + V_{2s} + V_{0s} \quad (9)$$

$$I_s = I_{1s} + I_{2s} + I_{0s} \quad (10)$$

$$I_{\text{sh}} = I_{1\text{sh}} + I_{2\text{sh}} + I_{0\text{sh}} \quad (11)$$

$$V_{pq} = V_{1pq} + V_{2pq} + V_{0pq}. \quad (12)$$

In the transmission system without UPFC, for a single phase-to-ground fault, the apparent impedance of distance relay can be calculated using the equation

$$Z = \frac{V_R}{I_R + \frac{Z_0 - Z_1}{Z_1}I_{R0}} = \frac{V_R}{I_{\text{relay}}} \quad (13)$$

where

V_R,I_R	phase voltage and current at relay point;
I_{R0}	zero sequence phase current;
I_{relay}	relaying current.

If this traditional distance relay is applied to the transmission system with UPFC, the apparent impedance seen by this relay can be expressed as

$$\begin{aligned} Z &= \frac{V_s}{I_s + \frac{Z_0 - Z_1}{Z_1}I_{s0}} = \frac{V_s}{I_{\text{relay}}} \\ &= nZ_1 + \frac{I_{\text{sh}}}{I_{\text{relay}}}(n-0.5)Z_1 + \frac{I_{0\text{sh}}}{I_{\text{relay}}}(n-0.5)(Z_0 - Z_1) \\ &\quad + \frac{V_{pq}}{I_{\text{relay}}} + \frac{I_f}{I_{\text{relay}}}R_f. \end{aligned} \quad (14)$$

In practice, one side of the shunt transformer is often based on a delta connection, and thus there is no zero sequence current injected by UPFC, that is to say $I_{0\text{sh}} = 0$, then the equation can be rewritten as

$$Z = nZ_1 + \frac{I_{\text{sh}}}{I_{\text{relay}}}(n-0.5)Z_1 + \frac{V_{pq}}{I_{\text{relay}}} + \frac{I_f}{I_{\text{relay}}}R_f. \quad (15)$$

From the above, it can be seen when the conventional distance relay is applied to the transmission system employing UPFC during the phase-to-ground fault, the apparent impedance seen by this relay has three parts: positive sequence impedance from the relay point to fault point, which is what the distance relay is set to measure; the second is due to the impact of UPFC on the apparent impedance, which can be further divided into two parts; one results from the shunt current I_{sh} injected by the STATCOM and another is the impact of the series voltage V_{pq} injected by the SSSC; the last part of the apparent impedance is due to the fault resistance.

It should be mentioned that the foregoing analysis is a theoretical analysis simply to illustrate the effect the UPFC has on the apparent impedance and hence on the performance of the distance relay.

B. Practical Consideration and Relay Modeling

As mentioned before, the primary system fault information is derived using the Matlab software. The digital simulation is run at 50 kHz. Both the CVTS and CTs have their own frequency responses and can therefore affect the voltage and current signals measured from the primary system. In the studies described here, these effects are incorporated into the simulation via the impulse responses of both the primary system transducers which in turn have been generated from frequency tests carried out on practical models of the equipments. Furthermore, a second-order Butterworth anti-aliasing filter with a cutoff frequency of 20 kHz has been incorporated. The digitization of the analogue information is achieved via a 16-bit A/D converter before the data is finally processed through the distance relay algorithm.

The distance relay performance is attained by means of a impedance chart (R/X diagram). On this chart, the characteristic curves of the limit of operation of the relay and the system impedance seen by the relay under specified operation conditions are plotted to the same scale.

The impedance protection used for these studies is based on a Mho distance characteristic with a positive sequence voltage polarization [8].

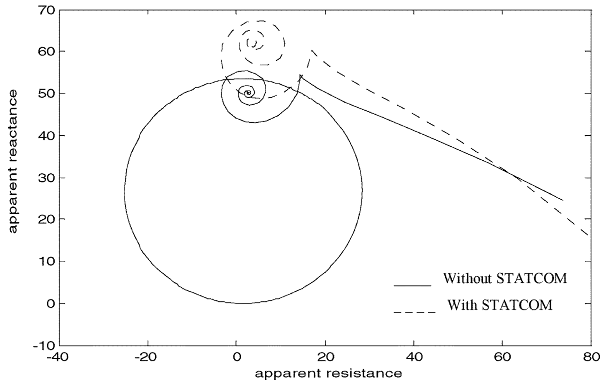

Fig. 6. Mho characteristic and apparent impedance trajectory with and without STATCOM.

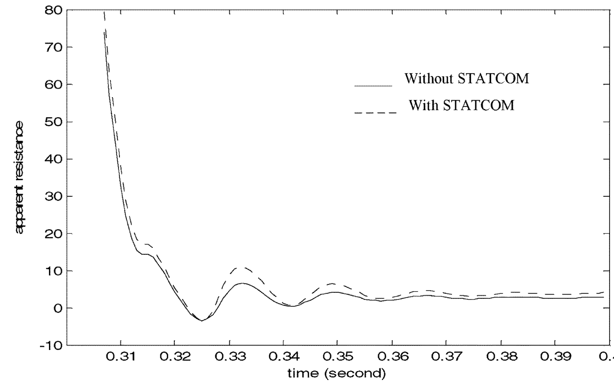

Fig. 7. Apparent resistance trajectory with and without STATCOM.

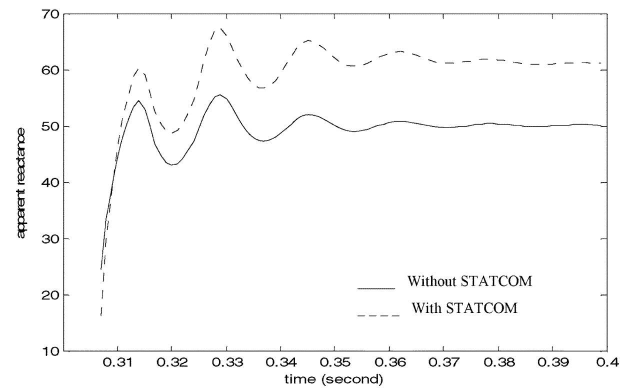

Fig. 8. Apparent reactance trajectory with and without STATCOM.

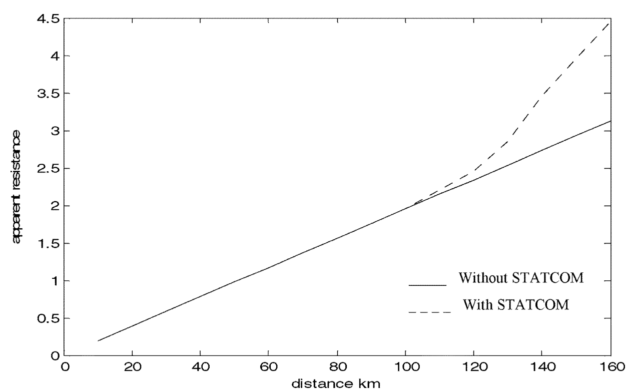

Fig. 9. Apparent resistance with different fault location.

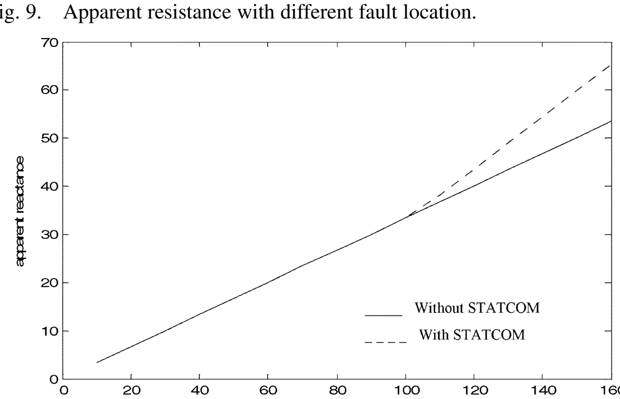

Fig. 10. Apparent reactance with different fault location.

IV. The Impact of STATCOM (Shunt Part of UPFC) on Distance Relay

There are three modes of operation of the UPFC; the first is when only the shunt voltage source inverter is connected to the UPFC system and it operates as STATCOM alone; the second is only when the series part is connected to the system and it operates as SSSC and thirdly when both parts work together it operates as the full UPFC system. When it is operated in the STATCOM mode, the main function is to regulate the connecting point voltage by injecting or absorbing reactive power into/from power system.

It is apparent from (15) that if the UPFC is operated as STATCOM and only a solid single phase-to-ground fault is considered, the equation becomes

$$Z = nZ_1 + (n - 0.5)Z_1 \frac{I_{\rm sh}}{I_{\rm relay}}. \tag{16}$$

The impact of STATCOM on the apparent impedance can be expressed using the ratio: $I_{\rm sh}/I_{\rm relay}$. In the following parts, the location of fault, the system source capacity and the setting of STATCOM will be considered. A Mho characteristic with a positive sequence voltage polarization is used as a zone one distance relay to cover 80% of the transmission line.

A. The Effect of Fault Location

When an A-ground fault is on the right side of STATCOM, i.e., at a fault distance of 150 km from the relay point, and the desired voltage $V_{\rm ref} = 1.0$ p.u., the apparent impedance trajectory seen by the A-ground element of the system with and without STATCOM together with the distance relay mho characteristic are as shown in Fig. 6; the corresponding apparent resistance and reactance, as a function of time, of the system with and without STATCOM are shown in Figs. 7 and 8, respectively.

From the above, it can be seen that both the resistance and reactance components of the transmission system apparent impedance with STATCOM are larger than for the system without STATCOM, the difference being more pronounced in the case of the reactance. A direct consequence of these differences is that the distance relay will underreach.

To study the coverage of the mho characteristic, faults at different positions have been studied, and the apparent resistance and reactance as a function of the fault location are shown in Figs. 9 and 10, respectively. It is apparent that when the fault is on the left side of STATCOM (i.e., < 100 km), the apparent

TABLE I
APPARENT IMPEDANCE AND THE RATIO OF $I_{\text{sh}}/I_{\text{relay}}$

Fault location	110	120	130	140	150	160
Apparent impedance	2.15+ j37.8	2.4+ j43	2.8+ j48.5	3.5+ j54	4+ j60.5	4.5+ j65
Influence ratio	0.48	0.52- j0.01	0.55- j0.02	0.6- j0.03	0.6- j0.03	0.62- j0.03

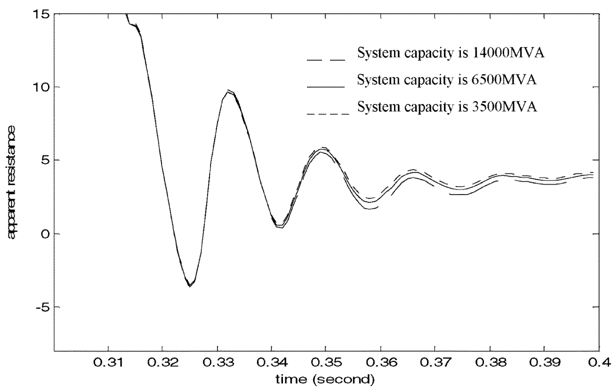

Fig. 11. Apparent resistance with different system capacity.

impedance seen by the distance relay is almost the same as that for the system without STATCOM; however, when the fault is on the right side of STATCOM, both the apparent resistance and reactance of the system with STATCOM are larger than for the system without STATCOM; this phenomena can be explained by the $I_{\text{sh}}/I_{\text{relay}}$ ratio as shown in Table I.

As can be seen from Table I, because of the reactive power injection by STATCOM, the voltage at the STATCOM connecting point is higher compared to the system without STATCOM, i.e., as seen by the distance relay, the fault is further away than the real distance; an increase in the apparent impedance will lead to the under-reaching of distance relay. Again as shown in Table I, the influence ratio increases with an increase in fault distance; this is so by virtue of the fact that for a remote fault, the relay current and STATCOM injecting current will decrease, but the variation in relay current is greater than in the injecting current.

When the STATCOM is installed in the middle of the transmission line (as is the case for the results shown in Figs. 6–10), and the original distance relay's cover range is 80% then, the relay coverage N_{new} for the system with STATCOM can be derived from the following:

$$50\%.Z_1 + (N_{new} - 50\%)\left(1 + \frac{I_{\text{sh}}}{I_{\text{relay}}}\right) Z_1 = Z_1.80\% \quad (17)$$

$$N_{new} = 50\% + \frac{30\%}{1+\frac{I_{\text{sh}}}{I_{\text{relay}}}}. \quad (18)$$

This equation clearly shows that the actual relay coverage is always less than the desired 80%. As an example for a ratio $I_{\text{sh}}/I_{\text{relay}} = 0.6$, the relay underreaching is approximate 12%.

B. The Effect of System Source Capacity

For different source capacities, the impact of STATCOM on a distance relay will also change. Figs. 11–13 show the apparent resistance, reactance, and STATCOM reactive injection

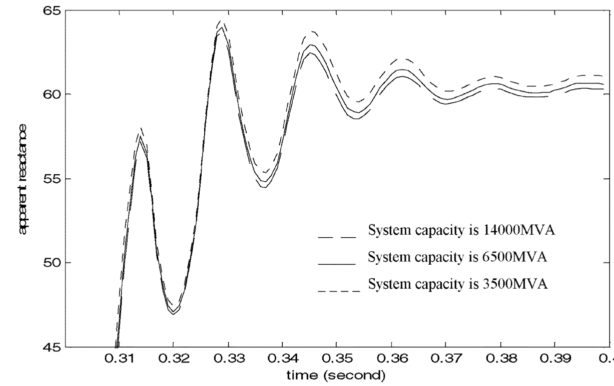

Fig. 12. Apparent reactance with different system capacity.

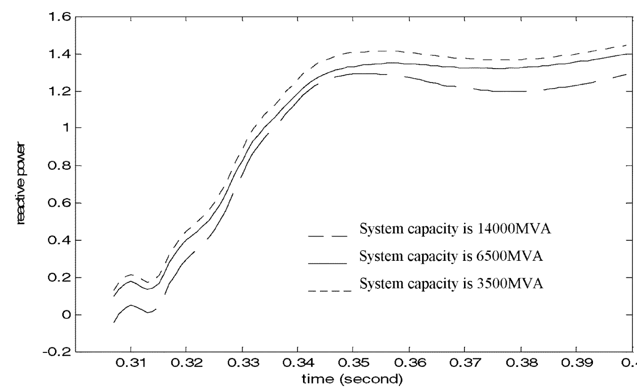

Fig. 13. Reactive power injection by STATCOM with different system capacity.

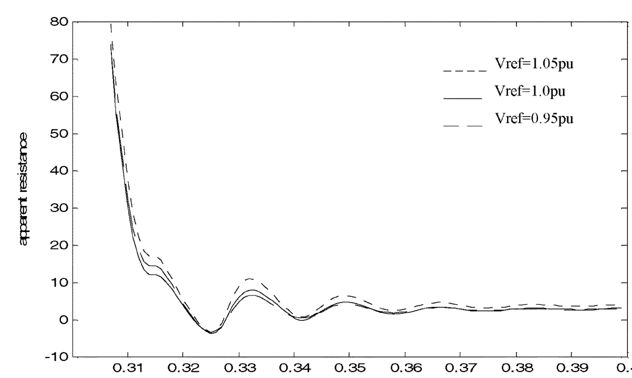

Fig. 14. Apparent resistance with different STATCOM setting.

according to system SCLs of 14 000, 6500, and 3500 MVA, respectively.

It is apparent that when a fault occurs on a relatively strong transmission system, the STATCOM will inject less reactive power to maintain the connecting point voltage at the requisite level and this leads to the apparent impedance seen by the distance relay being smaller in the stronger system compared to the system terminated in smaller SCLs.

C. The Effect of STATCOM Setting

Depending on different system conditions, STATCOM may have different setting values for the desired voltage, and this setting will also have an effect on the performance of distance relay. Figs. 14–16 show the apparent impedance and reactive

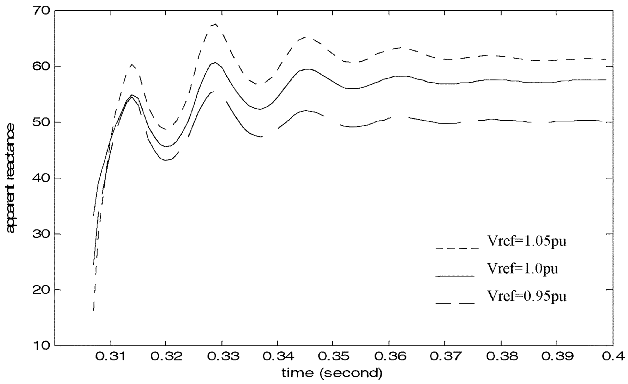

Fig. 15. Apparent reactance with different STATCOM setting.

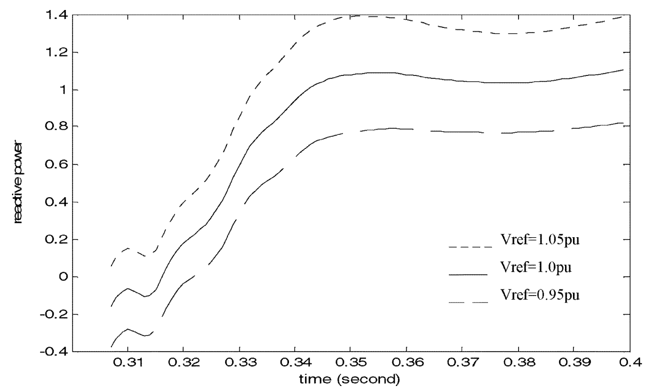

Fig. 16. STATCOM reactive power injection with different STATCOM setting.

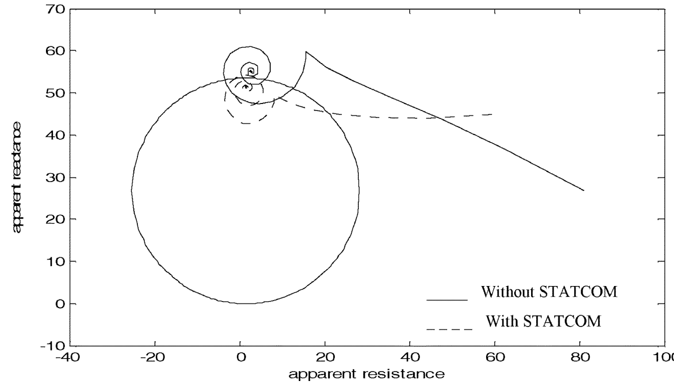

Fig. 17. Apparent impedance trajectory in the case of over-reaching.

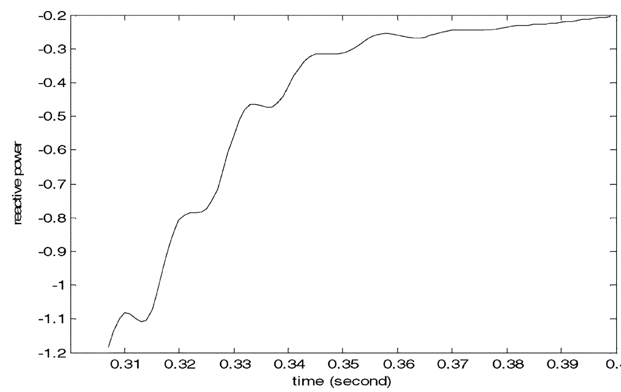

Fig. 18. Reactive power injection in the case of over-reaching.

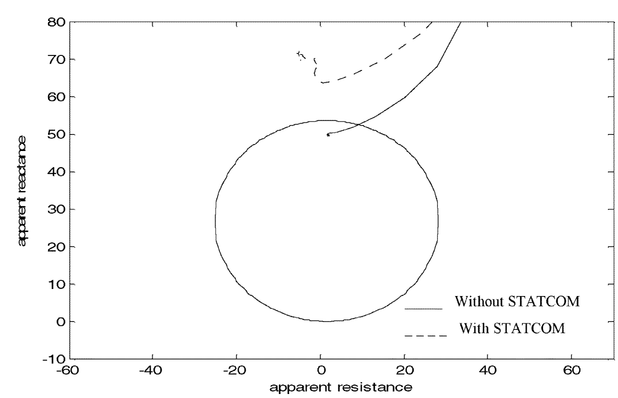

Fig. 19. Apparent impedance in B-C phase fault.

power injected by STATCOM during a single phase-to-ground fault when the STATCOM voltage settings are 0.95, 1.0, and 1.05 p.u., respectively.

When the setting voltage is high during a fault, the STATCOM will inject more reactive power to maintain the voltage at the desired level, i.e., $I_{\rm sh}$ is high; this inevitably increases the influence ratio resulting in the apparent impedance seen by distance relay increasing.

It is worth mentioning that under certain conditions, such as, for example when the system SCL is high, the voltage setting value is low and the fault is out-side the zone1 setting, the STATCOM connecting point voltage can exceed the original setting value; in this case, the STATCOM absorbs reactive power from the system causing a reduction in the apparent impedance as seen by the distance relay and hence a possibility of the relay overreaching which is clearly undesirable. This case can be seen from the results presented in Figs. 17–18 when the system SCL is 14 000 MVA and the STATCOM setting value is 0.9 p.u.

Fig. 17 shows the apparent impedance trajectory of the system with and without STATCOM when the fault is at the same location. As can be seen, for a single-phase earth fault at 165 km from the relay point (i.e., outside the 80% setting), the apparent impedance trajectory enters the mho boundary toward the end by virtue of the fact that during the fault, the STATCOM absorbs rather than injects reactive power from the transmission system.

D. The Effect of Phase-to-Phase Fault

During a phase-to-phase fault, the relay voltage input is line-to-line voltage and the current is delta line current. Figs. 19–21 show the apparent impedance seen by the distance relay during a B-C phase fault. The relay voltage is V_{BC} and the relay current is I_{BC}. The fault is a B-C phase fault at 150 km from the relay point, and the STATCOM voltage setting value is 1.0 p.u.

As can be seen from Figs. 20 and 21, during the fault, because of the presence of the STATCOM, the apparent reactance increases, but unlike the single phase-to-ground fault, the apparent resistance decreases. As a consequence, the distance relay sees this as an external fault as apparent from the impedance trajectory shows in Fig. 19.

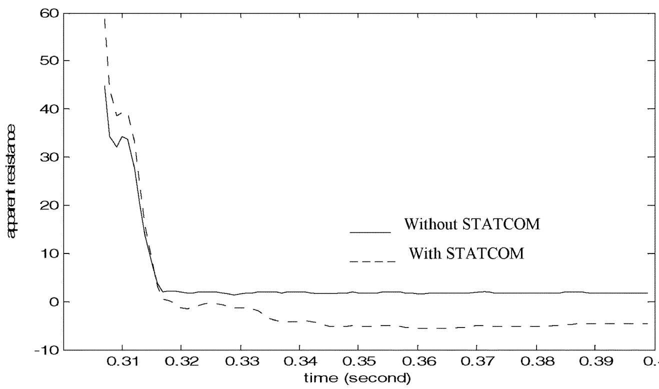

Fig. 20. Apparent resistance in B-C phase fault.

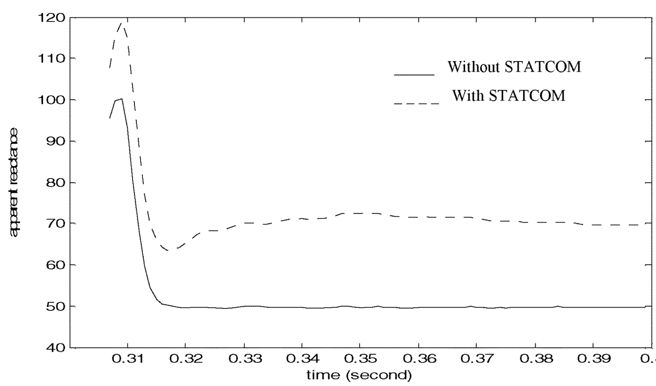

Fig. 21. Apparent reactance in B-C phase fault.

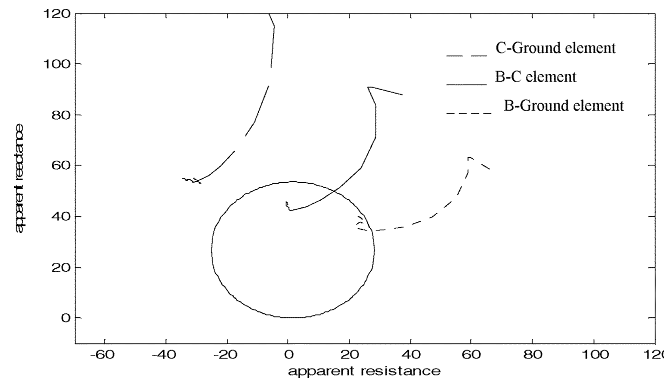

Fig. 22. Apparent impedance seen by different relay elements during B-C fault at 115 km.

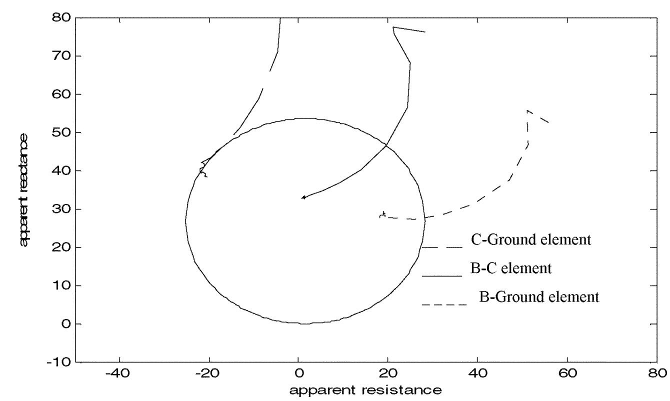

Fig. 23. Apparent impedance seen by different relay elements during B-C fault at 105 km.

Under certain conditions, for a phase-to-phase fault, both the phase-to-phase element and the single phase-to-ground relay elements will see the fault as an internal fault. This can be seen from Figs. 22 and 23; the fault is B-C phase fault at 115 km and 105 km from the relay point, respectively.

A series of studies have shown that for a B-C fault, both the B-ground and C-ground relay elements are adversely affected. Moreover, the maloperation of the C-ground element only occurs for a small range of fault distance values *viz.*, from about 100–105 km; and for B-ground element this range is 100-120 km.

Although not shown here, in the case of a B-C phase-to-ground fault, the results are very similar to the phase-to-phase fault i.e., there is a tendency for the distance relay to under-reach, and the phase-to-ground elements to maloperate, but the maloperation range of the phase-to-ground elements is bigger than the phase-to-phase fault i.e., for B-ground element this range is 100–130 km, for C-ground element this range is 100–115 km; in the case of a three phase fault, the apparent impedance seen all the three-phase elements increases, this will lead to the underreaching of distance relay.

E. Simulation Results and Conclusions for a System With STATCOM

1) During a fault, the apparent impedance will increase if the STATCOM supplies reactive power to the system, this will also result into the distance relay under-reach; the apparent impedance will decrease if the STATCOM consume the reactive power from the system, this will cause distance relay over-reach.
2) The setting of STATCOM has a significant impact on the apparent impedance. A higher voltage setting always results in a larger apparent impedance as compared to a lower voltage setting.
3) The influence ratio will increase with an increase in fault distance.
4) For a phase-to-phase fault, the apparent reactance increases but the apparent resistance may decrease, causing a possible under-reach.
5) For a phase-to-phase fault, the phase to earth element of the faulted phase may maloperate.

V. UPFC AND ITS INFLUENCE ON DISTANCE RELAY

When both the shunt and series parts work together, the UPFC works as a complete device and its function is to both regulate the power flow in the transmission line and maintain the voltage at the STATCOM connecting point. In this study, $V_{\rm ref} = 1.0$ p.u. and the active and reactive reference powers are set the same as for the system without UPFC. When there is an A-phase-to-ground fault at say 150 km, the simulation results show that the zero sequence component voltage of the UPFC is much higher than the positive and negative sequence components and this will dominate the relay point voltage and thus has a big impact on the apparent impedance; this can be directly

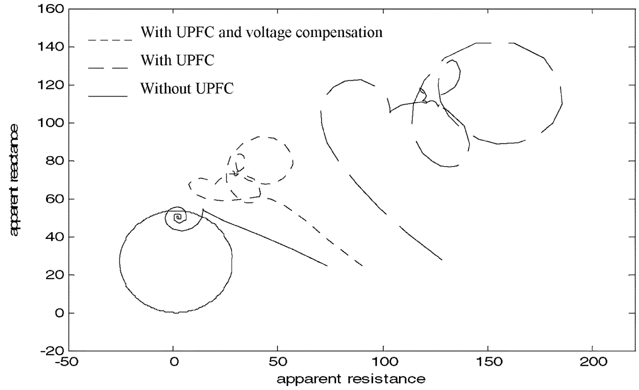

Fig. 24. Apparent impedance with and without voltage compensation.

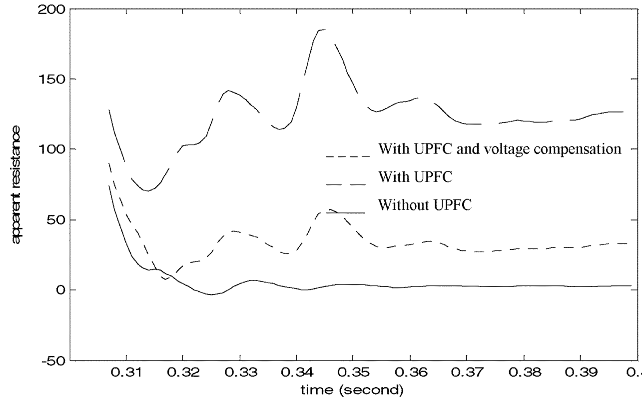

Fig. 25. Apparent resistance with and without voltage compensation.

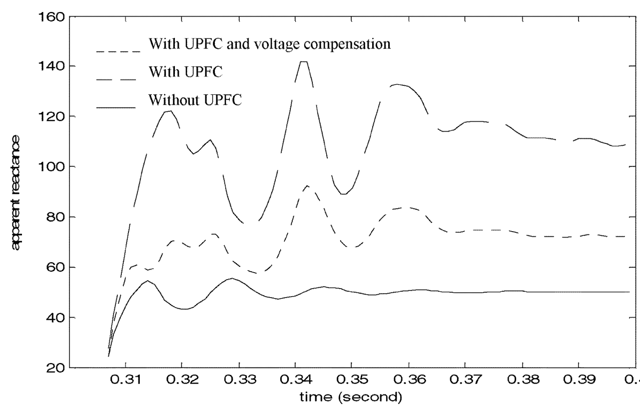

Fig. 26. Apparent reactance with and without voltage compensation.

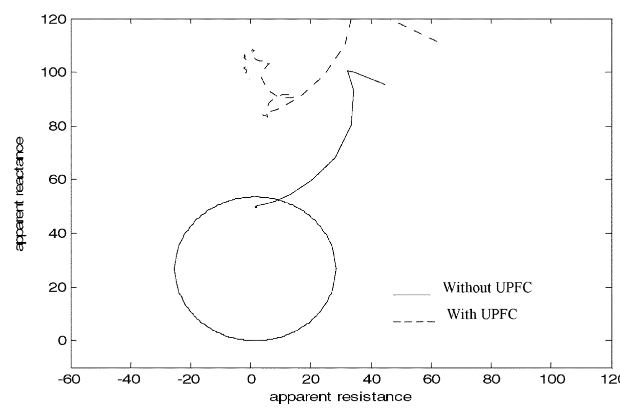

Fig. 27. Apparent impedance seen by B-C element with and without UPFC.

attributed to the presence of the magnetising branch of the series transformer in the faulted circuit, which in turn gives rise to a large zero sequence voltage component (this accentuates the relaying point voltage) associated with the injected voltage, in particular for a phase-ground fault.

If a compensation for the zero sequence voltage of UPFC V_{0pq} is introduced into the distance relay, then the relay voltage input V_s will be replaced by

$$V_s - V_{0pq} \tag{19}$$

where

V_{0pq} zero sequence voltage injected by the UPFC.

Using (15), the apparent impedance then becomes

$$Z = nZ_1 + \frac{I_{\rm sh}}{I_{\rm relay}}(n-0.5)Z_1 + \frac{V_{pq} - V_{0pq}}{I_{\rm relay}} + \frac{I_f}{I_{\rm relay}}R_f. \tag{20}$$

A. Single Phase-to-Ground Fault

Figs. 24–26 depict the apparent impedance seen by the distance relay for an A-earth fault at a fault distance 150 km from the relaying point. Comparing the impedance trajectory for a system with STATCOM (Figs. 6–8) and UPFC, it is apparent that the degradation in relay performance is far worse in the case of a system employing the full UPFC and as mentioned before, this can be directly attributed to the generation of a large zero-sequence voltage component in the injected voltage.

Fig. 24 also interestingly shows that if this zero sequence voltage component of the injected voltage (V_{0pq}) were to be known and the relaying point voltage V_s was then modified as $(\mathrm{V}_s' = \mathrm{V}_s - \mathrm{V}_{0pq})$, then the impedance trajectory shifts quite close to the relay Mho boundary.

Figs. 25–26 illustrate the variants in both the calculated resistance and reactance elements of the apparent impedance for the three conditions considered.

B. Phase-to-Phase Fault

When considering a B-C phase fault at 150 km, the apparent impedances seen by B-C relay element are shown in Figs. 27–29.

Like the case for a system with STATCOM, here again there is a tendency for the relay to under-reach and this is as a direct consequence of the calculated reactance and resistance components of the apparent impedance (in particular the reactance component) being significantly higher than is the case when there is no UPFC. Importantly, with the full operation of the UPFC, the impact on the apparent impedance is greater than when only the STATCOM is in use as evident from Figs. 19 and 27.

Fig. 30 shows that for a B-C phase fault at 105 km, both the phase-to-phase element and the B phase-to-ground relay elements will see the fault as an internal fault. Moreover, the maloperation of the B-ground element only occurs for a small range of fault distance values *viz.*, from about 100-115 km.

Although not shown here, in the case of a B-C phase-to-ground fault, the results are very similar to the phase-to-phase fault, i.e., there is a tendency for the distance relay to under-reach, and phase-to-ground elements to maloperate, but the maloperation range of the B-ground element is 100–125 km, which

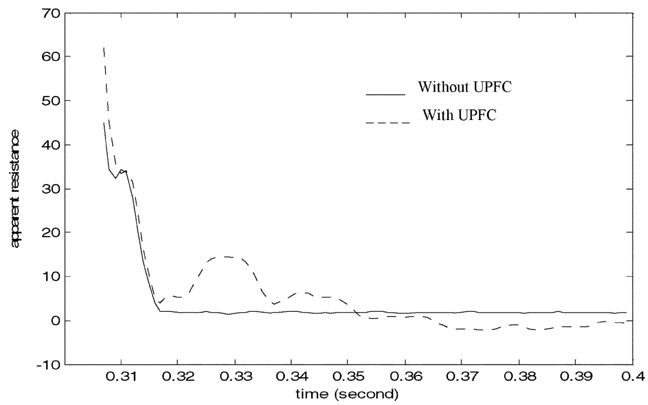

Fig. 28. Apparent resistance seen by B-C element with and without UPFC.

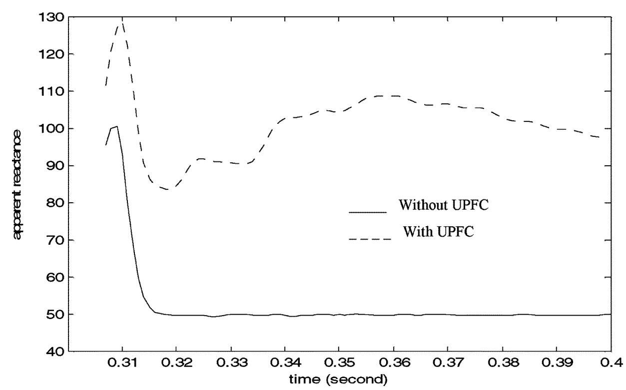

Fig. 29. Apparent reactance seen by B-C element with and without UPFC.

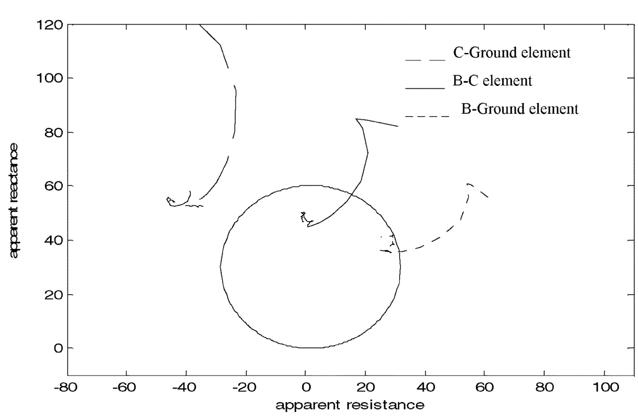

Fig. 30. Apparent impedance seen by different relay elements during B-C fault at 105 km.

is bigger than that for the phase-to-phase fault; in the case of a three phase fault, the apparent impedance seen by all the three phase elements increases; this will lead to the underreaching of distance relay.

C. Simulation Results and Conclusions for a System With UPFC

1) When SSSC part of the UPFC consumes active power, the apparent resistance will increase and when SSSC consumes reactive power, the apparent reactance will increase
2) Compared to STATCOM, UPFC has greater influence on the apparent resistance, this is due to the active power injection and consumption by both SSSC and STATCOM
3) For a phase-to-phase fault, there is a tendency for the distance relay to under-reach and also for the earth element to maloperate.
4) Compared to STATCOM, the impact of UPFC on the apparent impedance is much more significant and complex.

VI. SSSC and its Influence on Distance Relay

It should be mentioned that although not shown here (due to space consideration), the impact on the apparent impedance as seen by the distance relay is very similar between having the full UPFC (comprising both the STATCOM and SSSC) and the SSSC on its own in particular under the very commonly encountered single phase-to-ground faults. This is so by virtue of the fact that the magnetising branch of the series transformer of the SSSC is included in the faulted circuit in both cases and this in turn gives rise to a large zero sequence voltage component in the relay point voltage. As discussed before, this has a major impact on the apparent impedance. The STATCOM part of UPFC has a delta/Y transformer and therefore acts as a trap for the dominant zero sequence component in the current signals for faults involving ground and thus has very little influence on the apparent impedance when used in conjunction with the SSSC (as in the case for a UPFC).

The SSSC's impact on distance relay for a phase-to-phase fault is relatively simple: when the SSSC injects reactive power into the system, it is operated like a series capacitor and the apparent impedance decreases, when it consumes reactive power from the system, it is operated like a series inductance and the apparent impedance increases.

It should be mentioned that it is possible to inject active power into the system when an energy storage device is connected to the dc side of the SSSC, and studies associated with such a system will be part of the on-going work.

VII. Conclusion

This paper firstly presents a detailed model of a transmission system employing UPFC. Secondly, a calculation procedure for the apparent impedance of the system with UPFC for a single phase-to-ground fault is given; this is to illustrate the adverse effect the presence of a UPFC has on the performance of a distance relay. The simulation results show the impact of UPFC when it is operated as STATCOM and UPFC, respectively, on the distance relay. When the UPFC is operated as STATCOM, the apparent impedance is influenced by the reactive power injected/absorbed by the STATCOM, which will result in the under reaching or over reaching of distance relay. Importantly, the impact on the performance of a distance relay is significantly higher when the full UPFC is in operation compared to a system employing only the STATCOM part of the UPFC; this is by virtue of the fact that in the case of the former, there is active and reactive power injected by both STATCOM and the SSSC.

When comparing the results for a single-phase-earth and phase-phase faults, there is a tendency for the distance relay to under-reach more in the case of the latter and this is so for a system employing either STATCOM or the full UPFC. Furthermore, in the case of the phase-to-phase fault, there is a tendency for the distance relay earth fault element to pick up an external fault.

The results presented in this paper clearly highlight the fundamental problems of protecting a transmission system employing a UPFC using distance protection. Work is underway in extending the study for other types of system and fault conditions such as the effect of the location of UPFC on distance relay, other types of fault, including intercircuit faults. These will be reported in due course.

Moreover work is also underway to investigate the zero sequence component compensation in the voltage signal at the relay point in order to improve the performance of a distance relay as applied to a system employing UPFC.

REFERENCES

[1] N. G. Hingorani and L. Gyugyi, *Understanding FACTS Concepts and Technology of Flexible AC Transmission Systems*. New York: IEEE Press, 2000.
[2] Y. H. Song and A. T. Johns, *Flexible AC Transmission Systems*. New York: IEEE Press, 1999.
[3] A. G. Phadke, T. Hlibka, and M. Ibrahim, "Fundamental basis for distance relaying with symmetrical components," *IEEE Trans. Power App. Syst.*, vol. PAS-96, pp. 635–646, Mar./Apr. 1977.
[4] D. L. Waikar, S. Elangovan, and A. C. Liew, "Fault impedance estimation algorithm for digital distance relaying)," *IEEE Trans. Power Delivery*, vol. 9, no. 3, pp. 1375–1383, Jul. 1994.
[5] K. El-Arroudi, G. Joos, and D. T. McGillis, "Operation of impedance protection relays with the STATCOM," *IEEE Trans. Power Del.*, vol. 17, no. 2, pp. 381–387, Apr. 2002.
[6] P. K. Dash, A. K. Pradhan, G. Panda, and A. C. Liew, "Adaptive relay setting for flexible AC transmission systems (FACTS)," *IEEE Trans. Power Del.*, vol. 15, no. 1, pp. 38–43, Jan. 2000.
[7] W. G. Wang, X. G. Yin, J. Yu, X. Z. Duan, and D. S. Chen, "The impact of TCSC on distance protection relay," in *Proc. Int. Conf. Power System Technology (POWERCON '98)*, vol. 1, Aug. 1998, pp. 18–21.
[8] M. Khederzadeh, "The impact of FACTS device on digital multifunctional protective relays," in *Proc. IEEE/PES Transmission and Distribution Conf. and Exhib. 2002: Asia Pacific*, vol. 3, Oct. 6–10, 2002, pp. 2043–2048.
[9] G. Sybille and L.-H. Hoang, "Digital simulation of power systems and power electronics using the MATLAB/simulink power system blockset," in *Proc. IEEE Power Engineering Soc. Winter Meeting*, vol. 4, Jan. 4, 2000, pp. 2973–2981.
[10] K. K. Sen and E. J. Stacey, "UPFC-unified power flow controller: Theory, modeling, and applications," *IEEE Trans. Power Del.*, vol. 13, no. 4, pp. 1453–1460, Oct. 1998.

Xiaoyao Zhou received the B.S. and M.S. degrees from Hohai University, China, in 1996 and 1999, respectively. He is currently pursuing the Ph.D. degree in the Power and Energy System Group, University of Bath, Bath, U.K.

His current research interests are the electromagnetic transient modeling and simulation of power system and application of artificial intelligence to power system protection.

Haifeng Wang (M'96–SM'03) received the M.I.E.E.E., M.I.E.E., and C.Eng. degrees.

He is a Senior Lecturer, Department of Electrical and Electronic Engineering, University of Bath, Bath, U.K. His teaching and research speciality is power systems analysis and control.

Mr. Wang is a member of the IEE (U.K.).

R. K. Aggarwal (SM'91) received the B.Eng. and Ph.D. degrees from the University of Liverpool, Liverpool, U.K., in 1970 and 1973, respectively.

He joined the Power System Group at the University of Bath, Bath, U.K., where he is currently a Professor and Head of the Energy System Group. His main research interests are power system modeling and application of digital-technology and AI to protection and control. He has published over 300 technical papers and co-authored four textbooks.

Dr. Aggarwall is a Fellow of the IEE (U.K.).

Phil Beaumont (SM'04) received the B.Sc. (Hons.), C.Eng., and M.I.E.E. degrees.

He is an Engineering Director for Protection and Control within Toshiba International (Europe) Ltd. He is also a Chief Engineer within the Protection and Control Division of TMT&D Corporation, Japan. He is principally responsible for product development and technical marketing of protection and control systems.